International Journal of Microwave and Wireless Technologies

cambridge.org/mrf

Research Paper

Cite this article: Seah SJ, Jong SL, Yin Lam H, Leow CY (2024) The study of shadowing effect for LTE and 5G networks in suburban environment. *International Journal of Microwave and Wireless Technologies* **16**(2), 339–347. https://doi.org/10.1017/S1759078723001423

Received: 18 February 2023
Revised: 20 November 2023
Accepted: 21 November 2023

Keywords:
5G; air-to-ground; LTE; shadowing

Corresponding author: Siat Ling Jong;
Email: sljong@uthm.edu.my

The study of shadowing effect for LTE and 5G networks in suburban environment

Shi Jie Seah[1], Siat Ling Jong[1], Hong Yin Lam[2] and Chee Yen Leow[3]

[1]Faculty of Electrical and Electronic Engineering, Universiti Tun Hussein Onn Malaysia, Batu Pahat, Johor, Malaysia; [2]Faculty of Engineering Technology, Universiti Tun Hussein Onn Malaysia, Jalan Panchor, Johor, Malaysia and [3]Wireless Communication Centre, Faculty of Electrical Engineering, Universiti Teknologi Malaysia, Skudai, Johor, Malaysia

Abstract

The presence of obstacles in the propagation path is a critical factor in air-to-ground (AG) communication. The behavior of wireless signal propagation depends on several variables, such as frequency, building height, elevation angle, and street design. This paper aims to compare the three established line of sight (LOS) probability model based on actual site data, including the building geometry in suburban environment. The comparison between these three models using the site data provide a guideline for selecting the LOS probability model based on the optimistic and pessimistic predictions. The shadowing loss was evaluated at frequencies 2 and 3.5 GHz with an elevation angle of 20° in two suburban locations at Universiti Tun Hussein Onn Malaysia. Three prediction models, ITU-R P.1410-5, Holis and Pechac, and Pang et al., available in the literature were used to identify and compare the line-of-sight probability. By focusing on the shadowing model in suburban area, the guideline for optimizing LOS communications or navigation in these challenging environments can be developed. The finding highlights the importance of considering building height in AG communication for network performance evaluation and design.

Introduction

Recently, unmanned aerial vehicles (UAVs) have experienced significant growth in various industries because of their mobility, ease of deployment, and low cost. Due to the maneuverability of UAVs and blockage by ground structures such as buildings, the reliability of the line of sight (LOS) air-to-ground (AG) communication link can be unpredictable [1]. UAVs can be simply categorized as pertaining to the airborne layer, which falls into two types specifically, the low-altitude platform (LAP) and high-altitude platform (HAP). LAPs can stay at a few meters to tens of kilometers (km), whereas HAPs are made up of flying platforms like gas-filled balloons or aeroplanes that operate in the stratosphere at an altitude of roughly 20 km. Consequently, it is crucial to investigate the shadowing effect caused by the buildings and study the LOS probability for AG communication system performance evaluation.

In wireless propagation, the channel link is affected by the obstacles that exist in the environment. Man-made structures such as buildings, houses and towers, and vegetations such as trees may block or scatter the signal, causing shadowing, and reflection [2]. Therefore, when a network designers plan for a wireless network, the propagation condition between the transmitter (Tx) and receiver (Rx) should be taken into account. The propagation condition can be categorized into two main types: line-of-sight (LOS) and non-line-of-sight (NLOS). The LOS condition refers to where no obstacles exist between two points whereas the NLOS condition exists when there are obstacles between the Tx and Rx. The clearance between Tx and Rx can be examined by computing the probability of LOS. In AG communication, most researchers have studied airframe shadowing [3–6]. There are limited studies on the shadowing attenuation caused by building structures. In [7], the shadowing and path loss are characterized by considering the radio channel between UAVs and commercial long-term evaluation (LTE) base stations at the 800 MHz band in rural and hilly scenarios. Nathan et al. [8] evaluated the shadowing attenuation at two frequencies: 915 and 5760 MHz in rural area. However, no research has studied the effect of building structures on suburban setting at 2 and 3.5 GHz. Hence, this article aims to compare the three established LOS probability model to provide a guideline for selecting LOS probability model and the shadowing effect of building structures focused on suburban setting at a frequency of 2 GHz for LTE and 3.5 GHz for 5G networks is investigated. Since there is no comparison between these three models has been presented from the literature and the intention of this paper is not to find out the accuracy of the model but rather to compare the models in terms of to finding out the sensitivity of the model.

The rest of the paper is organized as follows. Second section summarized the background of the study, and the approaches and methodology used in this study are briefly explained in following section. The results and discussions of the LOS probability and shadowing attenuation are presented in next section. Finally, conclusions are drawn in last section.

Research background

The literature shows several methods available to determine the LOS probability. The standardized channel model 3GPP TR 38.901 [9] introduced the LOS probability calculation based on the massive measurement results. This model is available for different scenarios, including indoor and outdoor building environments. On the other hand, the ITU-R P.1410-5 [10] model suggested another approach, but it does not include the factor of building width. Since it has covered the range of UAV altitude and support the networking devices, such as the aerial base station, aerial relay, or aerial server, this model can be utilized for UAV communications even though it is general and valid for transmitter and receiver at any height [11]. Both 3GPP and ITU-R models have covered urban, suburban, and rural scenarios. Holis and Pechac [12] proposed another approach where the LOS probability was fitted with respect to the elevation angle for HAPs. Worth noting that only the high-altitude scenario with a height more than 1000 m was appropriate for this model. Pang et al. [13] derived a height-dependent LOS probability model that takes into account of geometric elements, including terminal placements, building height distribution, building width, and building space. In spite of that, this model does not include the factor of antenna pattern. Although this model is suitable for use at both low and high altitudes, but it performs better at high altitude. In [14], a geometry-based stochastic probability model was proposed. However, this model is more complex than the model proposed by Pang et al. [13] because it involved stochastic altitude-dependent and frequency-dependent probability models in the computation. Moreover, frequency-dependent LOS probability was also introduced by Xiang et al. [15] and Cui et al. [16] by considering frequency-related beamwidth. However, this method utilized numerical simulation of 4D environment which is more complicated to identify the LOS probability within the LOS clearance zone as compared to the previously mentioned existing models in [10, 12, 13], which depends on 2D and 3D environment. The details of each parametric model are explained in the following subsections.

3GPP TR 38.901 Model [9]

As mentioned earlier, the LOS probability model proposed by 3GPP is available for different environments, such as urban, suburban, rural, indoor hotspot factory, and indoor factory. For a suburban environment, the LOS probability, P_{LOS}, depends on the horizontal distance between the Tx and Rx, d_{2D} as given in equation (1). It is noted that this model was proposed based on an antenna height of 10 m in their measurement for a suburban environment.

$$P_{LOS} = \begin{cases} 1,\ d_{2D} \leq 18m \\ \frac{18}{d_{2D}} + exp\left(-\frac{d_{2D}}{36}\right)\left(1 - \frac{18}{d_{2D}}\right),\ 18m < d_{2D} \end{cases}. \tag{1}$$

ITU-R P.1410-5 Model [10]

According to International Telecommunication Union (ITU), the probability that a LOS link exists between a given Tx and Rx position is calculated by adding the probabilities that each building in the propagation path is lower than the height of the link interconnecting the Tx and Rx at the point where the link crosses the building. The height of the link connection at any point between Tx and Rx, h_{LOS}, is related as:

$$h_{LOS} = h_{tx} - \frac{d_{LOS}\left(h_{tx} - h_{rx}\right)}{d_{rx}}, \tag{2}$$

where d_{LOS} is the distance from the Tx to the obstacles, d_{rx} is the horizontal distance between Tx and Rx, h_{tx} and h_{rx} represent the height of Tx and the height of Rx, respectively. Furthermore, three main parameters are required in this model, which are the ratio of land area covered by buildings to the total land area, α which ranges from 0.1 to 0.8, the mean number of buildings per unit area, β ranges from 750 to 100, and the random variable determining the building height distribution, γ. The number of buildings between two points, b_r can be approximated as given in (3) if it is considered that structures are generally evenly spaced apart. Hence, the probability of LOS link exists at a location, $P_{LOS,\ d}$, can be computed as (4):

$$b_r = floor\left(d_{rx}\sqrt{\alpha\beta}\right), \tag{3}$$

$$\begin{aligned} P_{LOS,\ d} &= \prod_{j=0}^{i} P_j\ i \in \{0, \ldots, br - 1\} \\ &= 1 - e^{-\frac{h_i^2}{2\gamma^2}} \end{aligned} \tag{4}$$

where h_i is the height of the building that would obstruct the LOS link and can be calculated using the same equation of h_{LOS} given in (2). Details of the LOS probability computation of the ITU model can be found in [10]. Nevertheless, the LOS probability model is highly dependent on the height of Tx. This can be explained further with the graph displayed in Fig. 1. For instance, if the Tx is at a lower height, such as 1 km, the probability of LOS drops to 0% at a 77° elevation angle. This means that as the elevation angle increases, the number of buildings that obstructed the LOS link has become 1 in which the building is near to the Rx and the link is completely blocked by the structure. However, when the height of the Tx increases to 15 km, the link eventually would not be affected or blocked by the building.

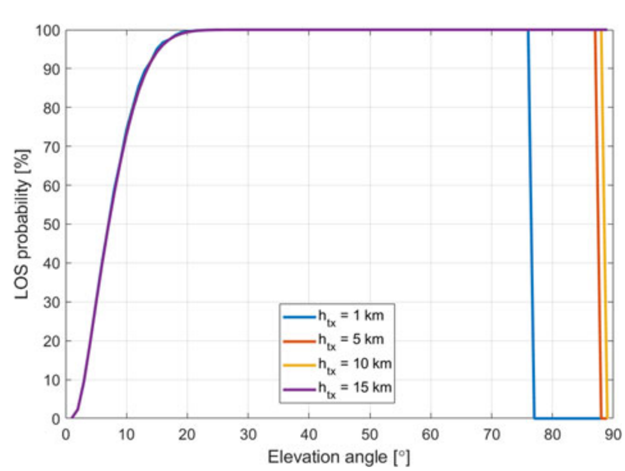

Figure 1. LOS probability affected by Tx height carried out with ITU model.

https://doi.org/10.1017/S1759078723001423 Published online by Cambridge University Press

Table 1. Empirical parameters for LOS probability calculation of Holis and Pechac model [12]

Environments	a	b	c	d	e
Suburban	101.6	0	0	3.25	1.241
Urban	120.0	0	0	24.30	1.229
Dense urban	187.3	0	0	82.10	1.478
Urban high-rise	352.0	−1.37	−53	173.80	4.670

Table 2. Empirical parameters for LOS probability calculation of Pang et al. model [13]

Environments	a_1	b_1	c_1	a_2	b_2
Suburban	1.698	1.082	30.07	38.63	0.4911
Urban	0.3891	1.098	23.92	21.31	0.4770
Dense urban	0.3475	1.018	20.15	18.87	0.4461
Urban high-rise	0.1885	0.9723	17.31	15.70	0.4106

Holis and Pechac Model [12]

An elevation-dependent probability model was proposed based on simulations using a randomly generated urban environment. This model targets mobile applications at 2, 3.5, and 5.5 GHz. The LOS probability as a function of elevation angle with empirical parameters based on environments can be written as:

$$P_{LOS}(\theta) = a - \frac{a-b}{1+\left(\frac{\theta-c}{d}\right)^{e}}, \tag{5}$$

where P_{LOS} is the LOS probability in percent, θ is an elevation angle in degrees, and a, b, c, d, e represent the empirical parameters of typical environments as given in Table 1.

Pang et al. model [13]

A height-dependent LOS probability model was proposed based on three-dimensional propagation characteristics of different environments for AG communications. This model improved the prediction method of the International Telecommunication Union Radiocommunication (ITU-R) standard by taking into consideration of geometric parameters and the measurement is taken from 0 to 1000 m, so it is suitable for both LAPs and HAPs. The derivation of this model is given in equation (6):

$$P_{LoS}(d_{RX}, h') = min\left(\frac{a_1 h'^{b_1} + C_1}{d_{RX}}, 1\right) \cdot \left[1 - exp\left(-\frac{d_{RX}}{a_2 h'^{b_2}}\right)\right] + exp\left(-\frac{d_{RX}}{a_2 h'^{b_2}}\right), \tag{6}$$

with P_{LoS} is the probability of LOS, d_{RX} is the horizontal distance from the Tx to the Rx, and h' is the difference between the height of Tx and the height of Rx ($h_{Tx} - h_{Rx}$). The empirical parameters a_1, b_1, c_1, a_2, b_2 are summarized in Table 2.

Theoretically, a signal propagating through an obstruction (or a building as shown in Fig. 2) on the propagation path will introduce a shadowing effect. Hence, it is important to study the shadowing effect caused by the obstacle along the propagation link. Knife-edge diffraction is a technique that is frequently used in propagation research to measure the amount of signal that has been obstructed within the shadowed region. Mountains or buildings are frequently depicted as knife-edges to evaluate the additional loss due to shadowing. Basically, knife-edge diffraction is a phenomenon when the signal is traveling from Tx, some of the signals are diffracted by the sharp edge of the obstacle to the shadow region. At the same time, the signal that is not cut off by the edge will continue to propagate. Figure 3 illustrates the phenomenon of knife-edge diffraction.

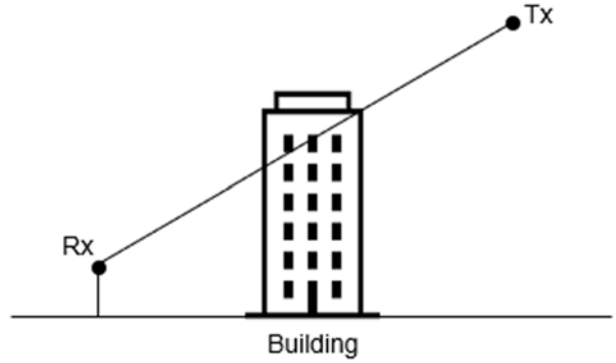

Figure 2. Model of simple building shadowing.

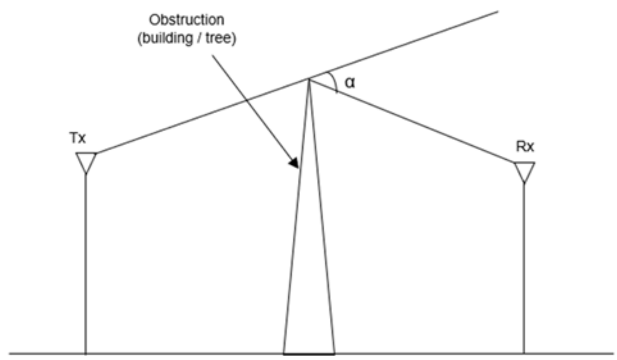

Figure 3. Knife-edge phenomenon.

An example of a simple building is the obstruction in Fig. 2 shows a signal transmitted from the right side to the left side of the mobile receiver on the ground. The model of a building can be represented by a screen as a protrusion on a knife-edge as shown in Fig. 4 [2]. The screen has been divided into three contiguous surfaces, namely Σ_1, Σ_2, and Σ_3, before the double integral of the Fresnel sine and Fresnel cosine function over the region can be calculated individually. The details of double integral Fresnel function can be found in [2]. The results of each integration will then be summed up consistently. More detailed geometric parameters are illustrated in Fig. 5 in order to have a clear understanding of the geometric parameters that would be used to calculate the horizontal, u, and vertical, v integration limits. These geometric parameters are given by the expression in (7):

$$\frac{y_0 - h_{RX}}{dd} = \tan(\theta), \quad x_0 = D\tan(\varphi), \quad dd = \frac{D}{\cos(\varphi)} \tag{7}$$

Thus, resulting

$$y_0 = \frac{D\tan(\theta)}{\cos(\varphi)} + h_{Rx}, \quad d_2 = \frac{y_0 - h_{Rx}}{\sin(\theta)} \tag{8}$$

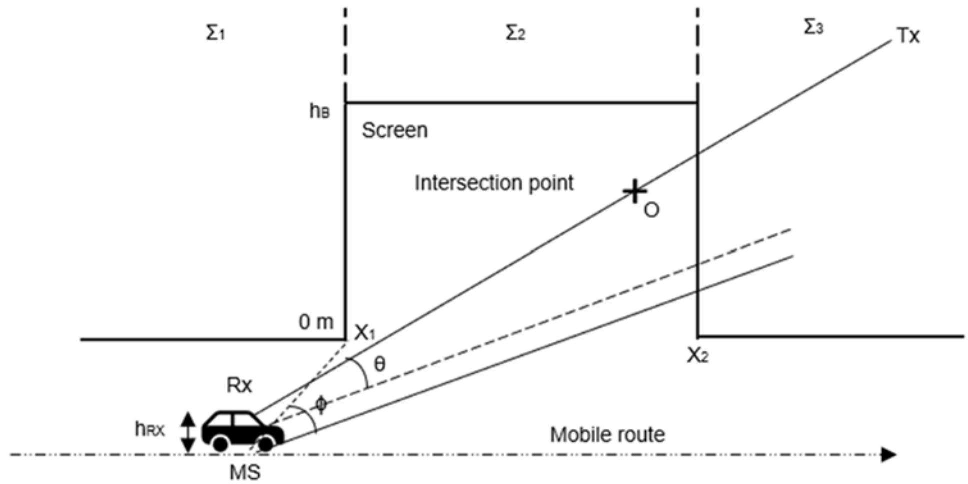

Figure 4. Model of a building as a protrusion [2].

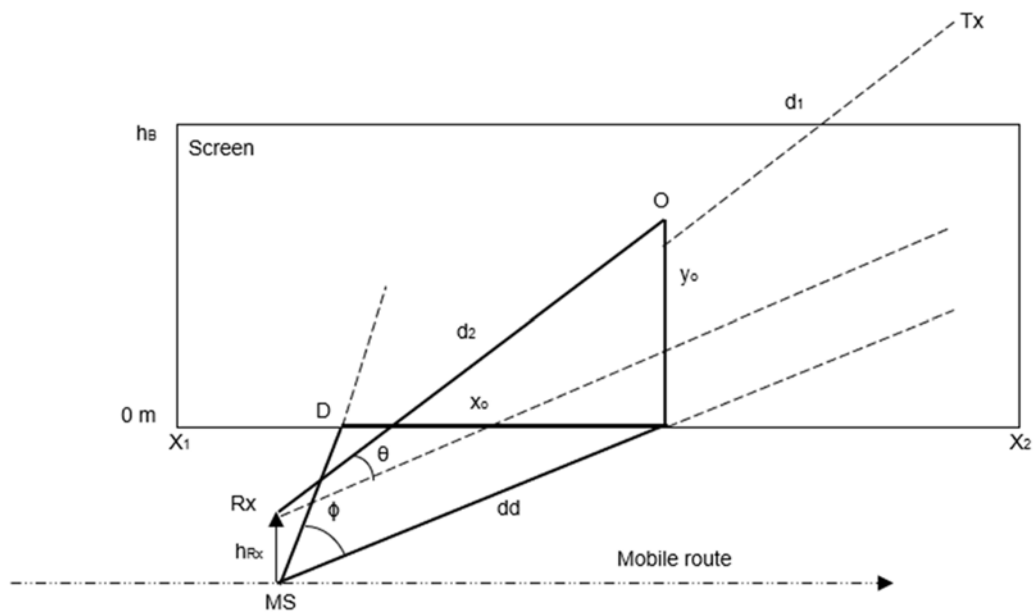

Figure 5. Detailed geometric parameters [2].

Referring to Fig. 5, assuming that the distance, d_1 from Tx to intersection point O is larger than the distance, d_2 from Rx to point O. Therefore, the first Fresnel zone radius can be expressed as:

$$R_1 = \sqrt{\lambda \frac{d_1 d_2}{d_1 + d_2}} \approx \sqrt{\lambda d_2}\,. \tag{9}$$

The calculation of integration limits for horizontal, u, and vertical, v, parameters for each surface can be found in [2]. Besides, the magnitude of the shadowing attenuation caused by obstacles in the radio path will be calculated using normalized field strength, E_{norm} which is given by:

$$E_{norm} = \frac{j}{2}(1-j)\int_{v1}^{\infty} exp\left(-j\frac{\pi}{2}v^2\right)dv\,. \tag{10}$$

According to Holis and Pechac [12], the shadowing loss can be analyzed by using a statistical approach in the form of a cumulative distribution function (CDF). It is expressed as:

$$P\left(L_s < x\right) = \frac{1}{2}\left[1 + erf\left(\frac{x-\mu}{\sigma\sqrt{2}}\right)\right](100 - P_{LOS}) + P_{LOS}, \tag{11}$$

where P is the probability in percent, L_s and x represent shadowing loss in dB, P_{LOS} is the LOS probability at street level computed from (5). The mean value, μ, and standard deviation, σ, in dB can be approximated from the normal distribution by (12):

$$\mu, \sigma = \frac{g+\theta}{h+i\theta}, \tag{12}$$

where θ is the elevation angle in degrees and g, h, i are empirical parameters which can be obtained from Table 3 to Table 5 for different frequencies, respectively [12]. It is important to take note that the empirical parameters are applicable for all environments.

Table 3. Empirical parameters for 2 GHz frequency [12]

	$0^\circ < \theta < 10^\circ$			$10^\circ \le \theta < 90^\circ$		
	g	h	i	g	h	i
μ	2.55	0.0594	0.0406	−94.20	−3.44	0.0318
σ	−12.96	−1.076	0.0780	−89.55	−8.87	0.0927

Table 4. Empirical parameters for 3.5 GHz frequency [12]

	$0^\circ < \theta < 10^\circ$			$10^\circ \le \theta < 90^\circ$		
	g	h	i	g	h	i
μ	2.70	0.059	0.0376	−92.90	−3.14	0.0302
σ	−12.24	−1.006	0.0788	−89.06	−8.63	0.0921

Table 5. Empirical parameters for 5 GHz frequency [12]

	$0^\circ < \theta < 10^\circ$			$10^\circ \le \theta < 90^\circ$		
	g	h	i	g	h	i
μ	2.636	0.0554	0.0352	−92.80	−2.955	0.0285
σ	−12.40	−0.998	0.0769	−89.54	−8.474	0.0900

Methodology

In this paper, two locations in a suburban environment are considered: they are Jalan Pembangunan 2 and Jalan Alfa 2 in Universiti Tun Hussein Onn Malaysia (UTHM) as shown in Figs. 6 and 7, respectively, were chosen to study the shadowing effects of building on NLOS connection. As discussed earlier in "Introduction" section, previous studies on shadowing effects focused on LTE signal at 800, 915, and 5760 MHz in rural scenario. According to Malaysian Communications Multimedia Commission (MCMC) [17], the 5G network in Malaysia would operates at a frequency of 3.5 GHz. Therefore, 2 GHz for LTE signal and 3.5 GHz for 5G network are chosen in this study. The CDF of shadowing loss has been calculated using equation (11). This study was primarily focused on the shadowing effects at the elevation angle of 20°. Additionally, based on the previous analysis of ITU model in Fig. 1 and the consideration of worst-case scenario, thus, the Tx height at 15 km and the minimum height of the Rx at 1 m were used in this study.

For the LOS probability model, three models that derived from the theoretical derivation, they are ITU-R P.1410-5 model [10], Holis and Pechac model [12], and Pang et al. model [13] were used in this study. 3GPP model is not considered as it is derived based on the measurement with specific parameters value which is not comparable with the model derived geometrically. The three main parameters of ITU-R model (α, β, γ) need to be obtained before

Figure 6. Location of the experiment site at Jalan Pembangunan 2: (a) real scenario and (b) Google map.

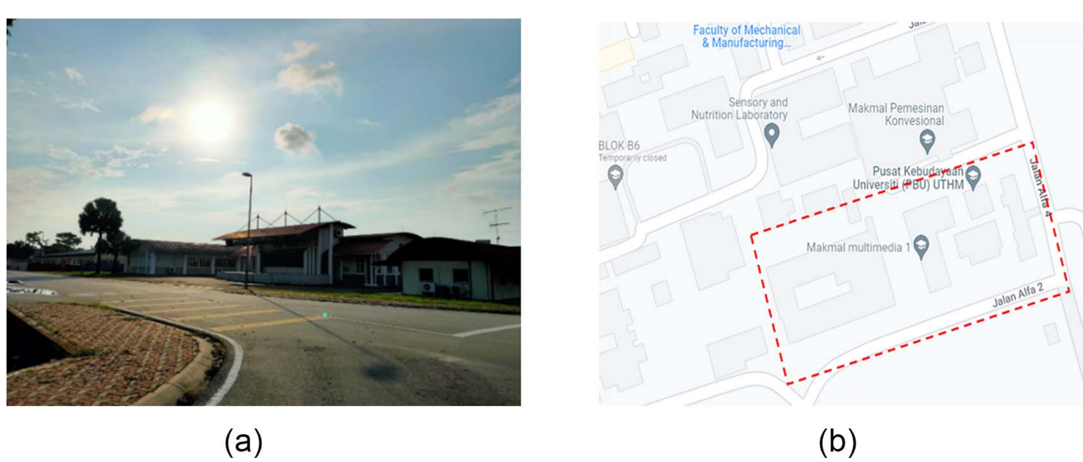

Figure 7. Location of the experiment site at Jalan Alfa 2: (a) real scenario and (b) Google map.

https://doi.org/10.1017/S1759078723001423 Published online by Cambridge University Press

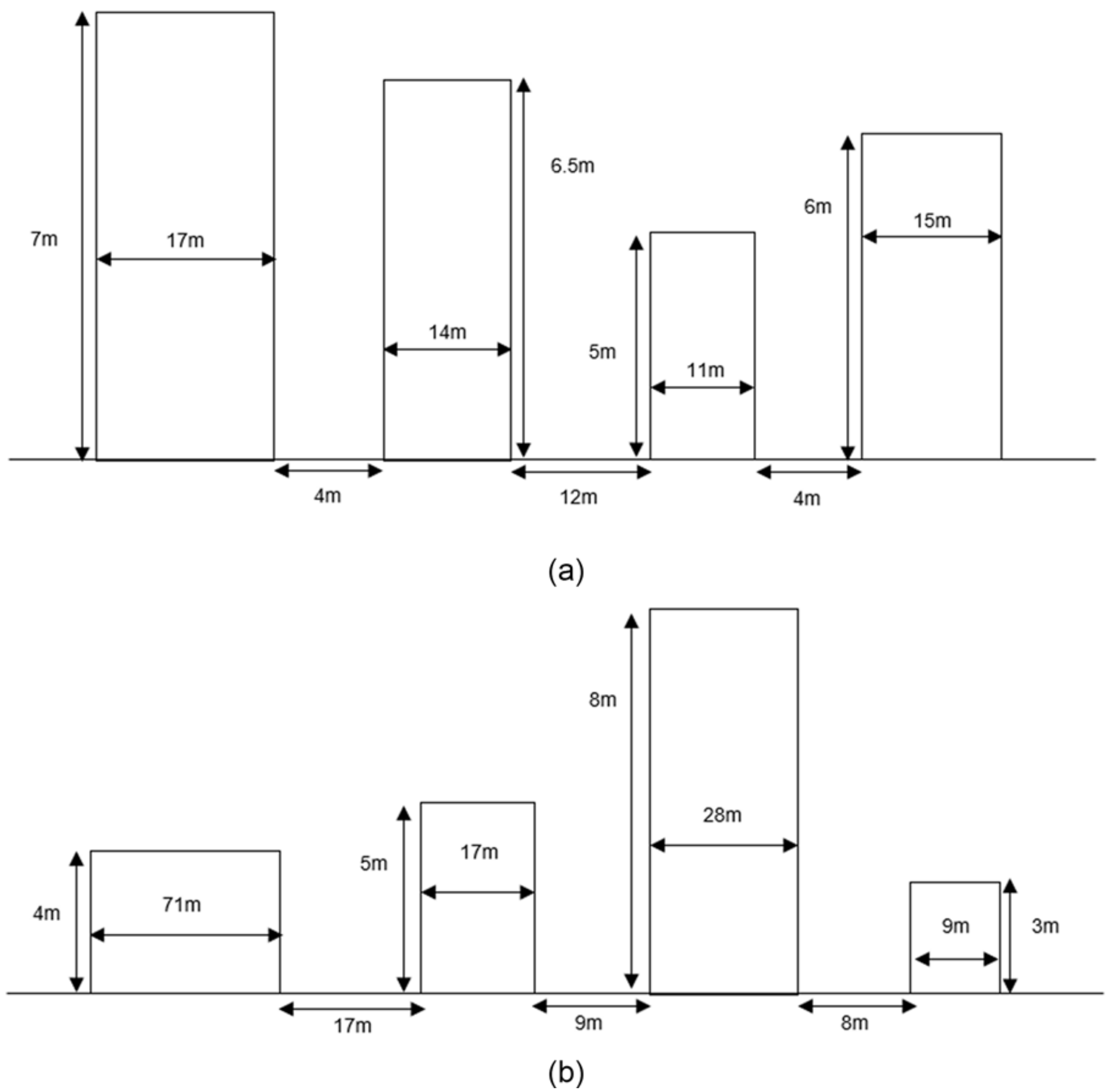

Figure 8. Building arrangement at: (a) Jalan Pembangunan 2 and (b) Jalan Alfa 2.

the LOS probability can be calculated. The α and β can be easily obtained from the 2-dimension view in Google map, whereas the parameter, γ, is obtained from the site survey which computes about 3.6 m per storey from the building. The information and building arrangement of each experiment site were given in Fig. 8(a) and (b).

Results and discussion

Figure 9 illustrates the LOS probability in a suburban environment. Simulation is computed for full angle elevation angle from 1° to 89° using ITU-R P.1410-5, Holis and Pechac model, and Pang et al. model. The result shows that the probability of LOS increases when the elevation angle increases. This indicates that the signal is transmitted in clear LOS without obstacles from Tx to Rx at a higher elevation angle. In addition, the LOS condition is met at an angle of 15° when Pang et al. and ITU-R P.1410-5 models are used while Holis and Pechac model increases slowly and steadily from 0° and finally reached 100% LOS condition at an 80° elevation angle.

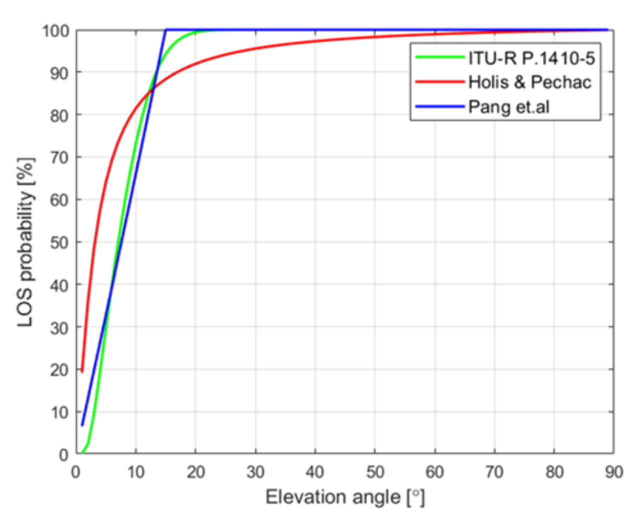

Figure 9. LOS probability of suburban environment.

https://doi.org/10.1017/S1759078723001423 Published online by Cambridge University Press

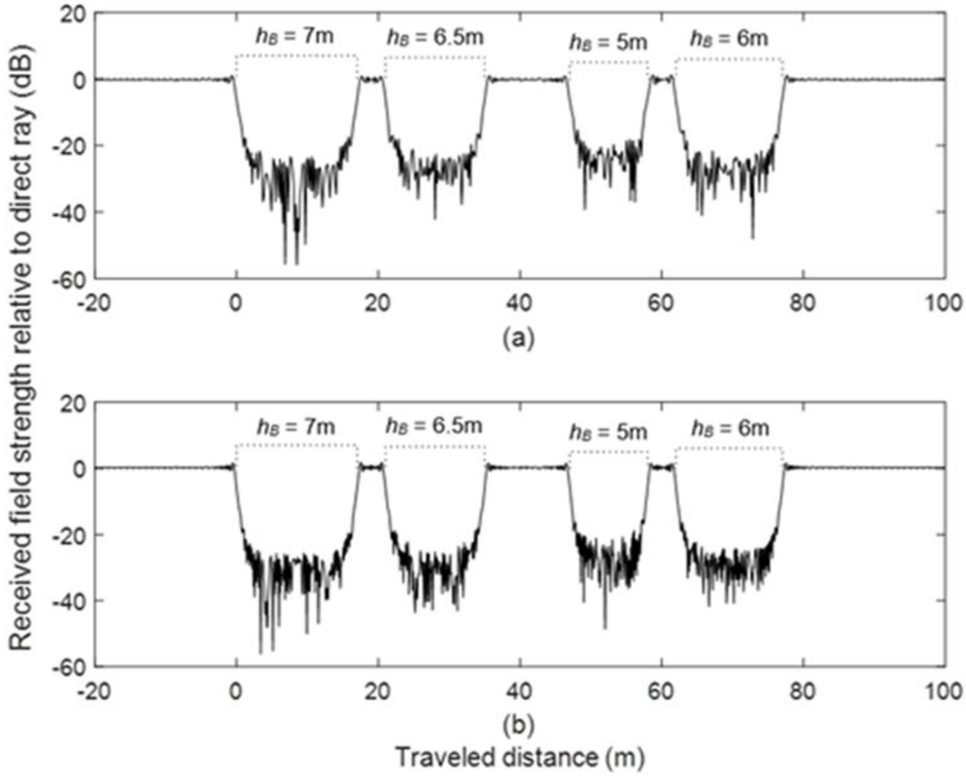

Figure 10. Shadowing effect along Jalan Pembangunan 2 at the frequency: (a) 2 GHz and (b) 3.5 GHz.

This difference is due to the fact that Pang et al. model is introduced for both LAPs and HAPs, and ITU-R P.1410-5 model is introduced for short path length propagation. On the contrary, Holis and Pechac model is suitable for HAPs only. It is observed that the Holis and Pechac model is more optimistic than ITU-R P.1410-5 model, followed by Pang et al. model at elevation angle less than 10°. However, at an elevation angle greater than 10°, Pang et al., and ITU-R P.1410-5 model are closely to each other and they are more optimistic than Holis and Pechac model as it has higher LOS probability. This means that Pang et al. and ITU-R P.1410-5 model can be selected for best case scenario, while Holis and Pechac model can be chosen when a worst-case scenario is considered.

The results of the NLOS shadowing effect for these two areas operating at frequencies 2 and 3.5 GHz are shown in Figs. 10 and 11. It is observed that when the building height, h_B is high, such as 7–8 m, the field strength is about −40 to −50 dB. The field strength increases to −20 and −35 dB when h_B is at 4 to 5 m. When h_B is 3 m, the field strength is less than −20 dB. Moreover, the received field strength is 0 dB when the signal is transmitted without being blocked by the building or other obstacles. This means that it is in LOS condition. In conclusion, the higher building will suffer stronger signal attenuation than the lower building heights.

The CDF of shadowing loss for frequency 2 and 3.5 GHz with an elevation angle of 10°, 20°, 30°, and 40° in a suburban environment was presented in Fig. 12. The probability of signal suffered from shadowing loss is high at the elevation angle of 10°. As the elevation angle increases to 20°, the probability of signal suffered from shadowing loss is decreased to 8%. A high elevation angle such as 30° and 40° as shown in Fig. 12 shows less probability of shadowing effect, which is lesser than 5%. This means that no impact of shadowing loss at a high elevation angle between Tx and Rx due to higher LOS probability. Moreover, it can be observed that the probability of signal suffered from shadowing loss at frequency 3.5 GHz is higher compared to the frequency at 2 GHz. However, the results in [12] indicate that the shadowing loss in a dense urban environment is still greater at an elevation angle of 50° to 60°. This indicates that the probability of LOS is lower, and resulting more shadowing loss in a dense urban environment.

Conclusion

In this paper, we conducted a thorough examination of the shadowing effects in the AG communication channel, focusing specifically on a suburban environment in Malaysia. While it is well-understood in the literature that building heights and elevation angles play a crucial role in determining the characteristics of the shadowing effects, our research adds context-specific details that are unique to the suburban setting we investigated.

We utilized three existing models: ITU-R P.1410-5, Holis and Pechac, and Pang et al., to estimate the probability of line-of-sight (LOS) connections between the transmitter (Tx) and the mobile receiver (Rx). Our simulation results revealed notable differences in the performance of these models. From the result, we can conclude that Pang et al. model achieved the LOS condition at lower elevation angles and was applicable for both LAPs and HAPs. On the other hand, the Holis and Pechac model was found to be suitable only for HAPs, achieving LOS at higher elevation angles. Lastly, the ITU-R P.1410-5 model presented a more optimistic performance compared to the Holis and Pechac model.

We have also presented the shadowing attenuations, assessed through the knife-edge diffraction technique, for two specific suburban locations in Malaysia: Jalan Pembangunan 2 and

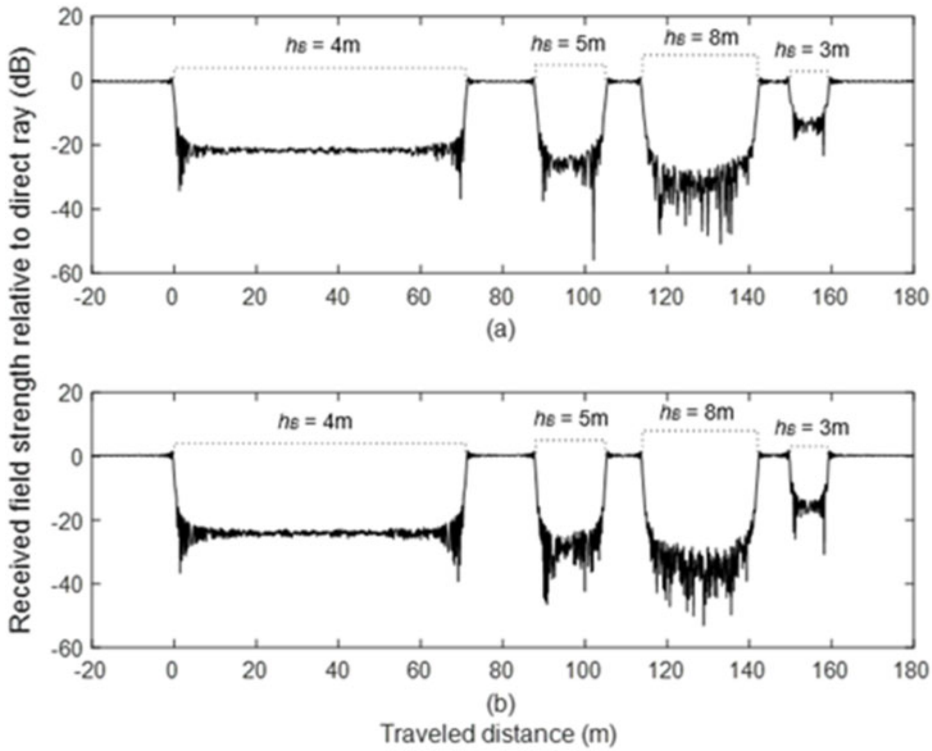

Figure 11. Shadowing effect along Jalan Alfa 2 at the frequency: (a) 2 GHz and (b) 3.5 GHz.

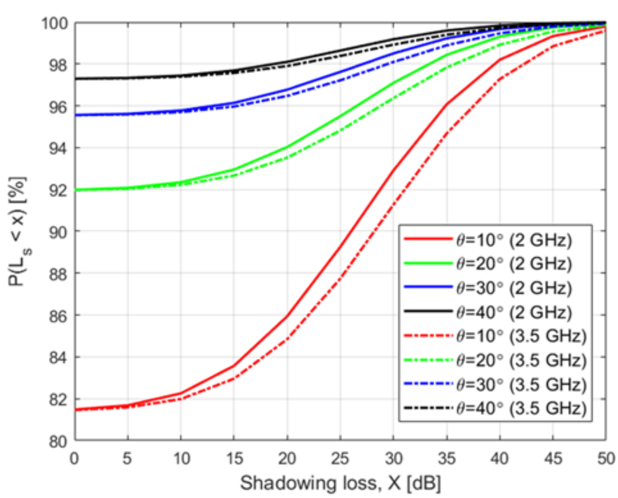

Figure 12. CDF of shadowing loss for a suburban environment at frequencies of 2 and 3.5 GHz.

Jalan Alfa 2, across two frequencies, 2 and 3.5 GHz. Our results indicated that the shadowing effect in the suburban environment under study was significant when the elevation angle was less than 30°.

While our findings reinforce the existing knowledge about the influence of building height and elevation angle on shadowing effects, they also provide specific insights into these effects in a unique, real-world context. As such, our study offers valuable data for radio network designers who need to evaluate network performance and optimize system design for AG communications in similar suburban environments.

Funding statement. This study was supported and funded by the Universiti Tun Hussein Onn Malaysia (UTHM) under TIER 1 Vot No. Q488, REGG Vot No. H885, and Ministry of Higher Education under CRG Vot No. K262. The work of C.Y. Leow was supported by Universiti Teknologi Malaysia under grant nos. 22H33, 08G83 and 05E07.

Competing interests. The authors report no conflict of interest.

References

1. **Khawaja W, Guvenc I, Matolak DW, Fiebig UC and Schneckenburger N** (2019) A survey of air-to-ground propagation channel modeling for unmanned aerial vehicles. *IEEE Communications Surveys and Tutorials* **21**(3), 2361–2391.
2. **Pérez Fontán F and Mariño Espiñeira P** (2008) *Modeling the Wireless Propagation Channel*. UK: John Wiley & Sons Ltd.
3. **Matolak DW and Sun R** (2017) Air-ground channel characterization for unmanned aircraft systems – Part III: the suburban and near-urban environments. *IEEE Transactions on Vehicular Technology* **66**(8), 6607–6618.
4. **Sun R, Matolak DW and Rayess W** (2017) Air-ground channel characterization for unmanned aircraft systems – Part IV: airframe shadowing. *IEEE Transactions on Vehicular Technology* **66**(9), 7643–7652.
5. **Meng YS and Lee YH** (2012) Study of shadowing effect by aircraft maneuvering for air-to-ground communication. *AEU – International Journal of Electronics and Communications* **66**(1), 7–11.
6. **Mielke DM, Schneckenburger N, Fiebig UC, Walter M and Bellido-Manganell M** (2021) Analysis of the dominant signal component of the air-ground channel based on measurement data at C-band. *IEEE Transactions on Vehicular Technology* **70**(4), 2955–2968.

7. **Amorim R, Nguyen H, Mogensen P, Kovács IZ, Wigard J and Sørensen TB** (2017) Radio channel modeling for UAV communication over cellular networks. *IEEE Wireless Communications Letters* **6**(4), 514–517.
8. **Nathan S, David WM and Alphan S** (2022) Measurement and modeling of low-altitude air-ground channels in two frequency bands. In *2022 Integrated Communication, Navigation and Surveillance Conference (ICNS)*, May, 1–10.
9. **Zhu Q, Wang C, Hua B, Mao K, Jiang S and Yao M** (2021) 3GPP TR 38.901 channel model. In Tafazolli R, Chatzimisios P and Wang C-L (eds), *Wiley 5G Ref: The Essential 5G Reference Online*. UK: John Wiley & Sons, Ltd, 1–35.
10. ITU-R P.1410-5 (2012) Propagation data and prediction methods required for the design of terrestrial broadband radio access systems in a Frequency Range from 3 to 60 GHz.
11. **Song M, Huo Y, Liang Z, Dong X and Lu T** (2022) Air-to-ground large-scale channel characterization by ray tracing. *IEEE Access* **10**(December), 125930–125941.
12. **Holis J and Pechac P** (2008) Elevation dependent shadowing model for mobile communications via high altitude platforms in built-up areas. *IEEE Transactions on Antennas and Propagation* **56**(4), 1078–1084.
13. **Pang M, Zhu Q, Bai F, Li Z, Mao K and Tian Y** (2021) Height-dependent LoS probability model for A2G Mm wave communications under built-up scenarios. *Computer Science* **878**, 1209–1217.
14. **Pang M, Zhu Q, Wang C-X, Lin Z, Liu J, Lv C and Li Z** (2023) Geometry-based stochastic probability models for the LoS and NLoS paths of A2G channels under Urban Scenarios. *IEEE Internet of Things Journal* **10**(3), 2360–2372.
15. **Xiang L, Jing X and Hongying T** (2018) Analysis of frequency-dependent line-of-sight probability in 3-D environment. *IEEE Communications Letters* **22**(8), 1732–1735.
16. **Cui Z, Guan K, Briso-Rodriguez C, Ai B and Zhong Z** (2020) Frequency-dependent line-of-sight probability modeling in built-up environments. *IEEE Internet of Things Journal* **7**(1), 699–709.
17. Malaysian Communications and Multimedia Commission (2019) Allocation of spectrum bands for mobile broadband service in Malaysia. https://www.mcmc.gov.my/skmmgovmy/media/General/pdf/PI-Allocation-of-spectrum-bands-for-mobile-broadband-service-in-Malaysia_1.pdf (accessed 21 August 2022).

Shi Jie Seah graduated from Universiti Tun Hussein Onn Malaysia in 2018 with a Bachelor of Electronic Engineering majoring in communication and in 2021 with a Master of Electrical Engineering. She is presently pursuing her Ph.D. degree in Electrical Engineering at Universiti Tun Hussein Onn Malaysia. Currently, she is a researcher for wireless propagation, and unmanned aerial vehicle (UAV).

Siat Ling Jong received her Bachelor's degree in Electrical Engineering from Universiti Tun Hussein Onn Malaysia (UTHM) in 2007. After that, she obtained a scholarship to pursue her Master's and Doctorate degrees in Electrical and Communication Engineering in the field of radio wave propagation for satellite communication systems at Universiti Teknologi Malaysia (UTM) in 2009 and 2015, respectively. In 2007, she joined UTHM as an assistant lecturer. In 2012 and 2013, she obtained a research attachment grant to Politecnico di Milano, Milan, Italy to do her research on rain effects and fade dynamics on satellite communication links. Since 2015, she has been a lecturer of Electronic Communications at UTHM. Her research interests include rain attenuation, radio wave propagation for a satellite communication system and atmospheric science, statistical modeling, unmanned aerial vehicle (UAV) communication and the Internet of Things (IoTs).

Hong Yin Lam received his Ph.D. in 2013 from the University of Technology Malaysia. He was awarded a Young Scientist Award at the International Symposium on Antennas and Propagation (ISAP), Japan, in 2012 and the Asia Pacific Radio Science Conference, Taiwan, in 2013. He has been working at the University of Tun Hussein Onn Malaysia since 2015. He has authored and co-authored more than 30 papers in international journals and conference proceedings and his current research interests include radiowave propagation for satellite communication and terrestrial application as well as photovoltaic system.

Chee Yen (Bruce) Leow (S′08-M′12-SM′21) is currently an Associate Professor with the School of Electrical Engineering, Faculty of Engineering and a Research Fellow with the Wireless Communication Centre, Universiti Teknologi Malaysia (UTM). He obtained a PhD degree in Wireless Communications from Imperial College London in September 2011 and a B.Eng. degree in Computer Engineering from UTM in June 2007. Dr Leow's current research interest includes non-orthogonal multiple access, drone communication, intelligent surfaces, advanced MIMO, millimeter wave communication, and prototype development using software defined radio, for beyond 5G and Internet of Things applications. His IEEE journal papers won the IEEE Malaysia Comsoc/VTS Joint Chapter's Best Paper Awards 2016, 2017, and 2021, and IEEE Malaysia AP/MTT/EMC Joint Chapter's Best Paper award 2017, 2018, and 2020. He is among the pioneers for 5G initiatives in Malaysia to promote 5G R&D collaboration between industry and academia.